

NAVAL SHIP STABILITY GUIDELINES: DEVELOPING A SHARED VISION FOR NAVAL STABILITY ASSESSMENT

D E Perrault, Defence Research & Development Canada – Atlantic, Canada

T Hughes, Salvage Division, SMIT International,, The Netherlands

S Marshall, Surface Ship Hydromechanics, Directorate of Sea Systems, MoD, UK

(DOI No: 10.3940/rina.ijme.2010.a3.173)

SUMMARY

Surface combatants are required to operate in conditions of high military threat and be capable of deployment to any area of conflict or crisis at any time. This requirement calls for the vessel and crew to be capable of safely contending with the full range of environmental conditions that may be encountered while pursuing their primary objective. Achieving and maintaining this capability is strongly influenced by the application of naval stability standards, many of which have a common origin, based on experiences from the World War II and before. Although such standards have apparently served the navies admirably over many years, there are many reasons to question their limitations and applicability in the context of modern ship design and procurement. This paper presents the efforts to date of the Naval Stability Standards Working Group to investigate the relationship between existing intact stability standards and capsized risk with respect to frigate forms.

NOMENCLATURE

The following are the major symbols used:

GZ	Righting lever arm (m)
ϕ	Roll angle (deg., rads in figures only)
GM	Metacentric height
Δ	Displacement
KG	Vertical centre of gravity (a.k.a. VCG)
L	Ships length at the design waterline (m)
λ	Ships length at the actual waterline (m)
$A_{\phi_1 - \phi_2}$	Area under the GZ curve defined by a range of roll angles, ϕ_1 to ϕ_2 . (m-rads)
V_s	Ship speed (m/s)
β	Ship heading with respect to the unidirectional wave system (deg.)
H_s	Significant wave height (m)
T_p	Peak wave period (s)
$P(X), p(X)$	Probability of X occurring
$P(X Y)$	Probability of X occurring given that Y has occurred
R_{adj}^2	Adjusted correlation coefficient; i.e., adjusted for degrees of freedom in the model used

See tables and appendix for a complete list of symbols.

The following are important roll angles:

ϕ_{SE}	Angle of static equilibrium (deg.)
ϕ_{VS}	Angle of vanishing stability (deg.)
ϕ_{RB}	Roll back angle (deg.)
ϕ_{DF}	Down-flooding angle (deg.)
$\phi_{Critical}$	User-defined angle of importance (deg.)

1. INTRODUCTION

The maintenance of a maritime strategic capability demands the ability to rapidly deploy to any area of conflict or humanitarian crisis. The time honoured naval expressions like “Any ocean. Any time.” reflect the

demands on vessel and crew to perform even in the face of high risk from military or environmental threats.

Since man set to sea, the strategy employed to reduce the risk to life presented by heavy weather has been to avoid it whenever possible. The advent of meteorological satellite technology has enabled the world’s commercial fleets in particular to make increasingly better use of this strategy to reduce the risk to vessel, crew, cargo, and environment. This operating philosophy of weather routing has been highly beneficial to the shipping industry. It has allowed the development and adoption of rationalised assignment (route) driven design and safety approaches. The strategy works optimally if the vessel continues to operate in the same role and specific environment against which it was designed.

In complete contrast, the design and operating philosophy for naval combatants is driven by the demand for strategic capability, particularly that which is realized through rapid deployment to any area at any time. This clearly means that it is not always possible to avoid high threat and extreme environmental conditions; rather, naval vessels and their crews must be capable of safely contending with them.

The attainment and maintenance of this capability is strongly influenced by the application of naval stability standards. Over half a century of warship design and operational experience has led many navies to adopt and apply very similar standards to the design process and for life-cycle management.

These stability standards have apparently served the navies admirably over the last forty years or so; they appear to have resulted in warship designs having a low level of capsized risk. Despite this apparently good service there are many reasons to investigate their validity and applicability, including:

- The level of safety assured by compliance with such standards is unknown.
- Modern naval hull forms are becoming increasingly less similar to those against which such standards were originally developed.
- A dynamic capsize is caused principally by seaway and wind excitation on a moving vessel, or as a function of time. The loss of stability may occur under a variety of conditions (intact or damaged) once the forcing function exceeds the available restoring force. It is questionable whether the essentially static measures truly reflect the dynamic behaviour in extreme conditions.

In light of recent advances in computational capability, hydrodynamic techniques and risk assessment methods, it is clear that the necessary investigation of these issues is now possible.

Recognising this, the Naval Stability Standards Working Group (NSSWG) was formed to develop a shared view on the future of naval stability assessment and develop a draft set of stability guidelines which can be utilised by the participating navies at their discretion.

It is foreseen that the investigation into stability of intact ships will be broken down into three consecutive stages. The first stage is an investigation into the relative merits of various measures for indicating the probability of extreme dynamic behaviour, and therefore risk of exceeding a critical roll angle which may be associated with a capsize. The second stage is to assess the level of safety currently accepted through the application of the existing naval standards. The third stage will integrate the effects of operator intervention.

This document is a summary record of the work done to date to investigate the relative merits of various selected measures for indicating the probability of extreme dynamic behaviour with respect to frigate type vessels. This work therefore concentrates on exposing the strengths and weaknesses of various parameters, many of which are part of the current naval standards. The results of this investigation will support the development of guidance on the ability of various measures of stability to truly reflect dynamic stability. It is expected to contribute to the development of suitable alternative approaches for assessment of dynamic stability as well.

2. BACKGROUND

2.1 STATIC CAPSIZE

A static capsize may occur suddenly when a disturbance is encountered that is sufficient to overcome the ship's inherent ability to remain in an equilibrium state at or near upright. The event has traditionally been characterized by parameters which relate to a reduction in the righting arm lever (or GZ curve, see Figure 1)

which represents the static stability of a vessel independent of forward speed and time. Conditions that could lead to static capsize include improper loading, lifting or topside icing (increasing VCG); towing, wind, or load shift, (increasing heel angle); trapped fluids on deck (increasing free surface effects); and loss of watertight integrity (loss of buoyancy/waterplane area).

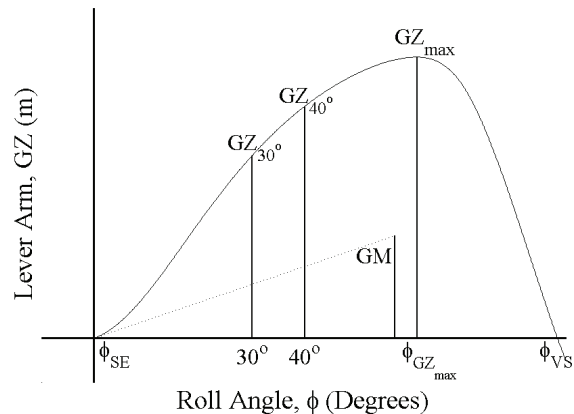


Figure 1. Typical Righting Arm (GZ) Curve.

2.2 DYNAMIC CAPSIZE

A Dynamic Capsize is caused principally by seaway and wind excitation on a moving vessel or as a function of time. This wind and wave action may lead to equipment damage, personnel injury, loss of system functionality and/or weather-tight/watertight integrity due to which the ship is unable to maintain its intact upright state. A dynamic capsize is characterized as a time-dependent event occurring in unrestrained 6 degrees of freedom motion. The loss of dynamic stability may occur under a variety of conditions (intact or damaged) once the forcing function exceeds the available restoring force. The capsize mode is often one of several main phenomena. Note that some of them can occur sequentially or in combination, ultimately leading to capsize.

2.2 (a) Sympathetic Rolling

Generally occurs in stern or stern-quartering seas with greater risk when travelling at or near the wave group velocity. There are two general types of dynamic rolling characterized by their time to occur:

- 1) Asymmetric resonant behaviour: The roll behaviour is asymmetric in nature and builds with each wave encounter. There are large amplitude oscillations in roll (as well as surge, sway and yaw motions) which occur as the result of fluctuations in the righting arm with the slow passage along the ship of long steep waves.
- 2) Sudden extreme behaviour: This mode of capsize is generally due to a sudden loss of transverse waterplane area and righting ability when a wave

crest is at or near amidships. Rolling motions coupled with the loss of transverse hydrostatic stability lead to capsize.

2.2 (b) Resonant Excitation

This mode of capsize occurs in beam seas when a ship is excited at or close to its natural roll period.

2.2 (c) Parametric Excitation

This mode of capsize is predominantly a following seas phenomena, but it can also be observed in head seas at low forward speeds. It is the periodic variation of the righting arm and buoyancy distribution which results in a gradual build up of excessively large roll angles at the same natural roll period as the vessel. These roll oscillations are most critical when the wave encounter frequency¹ is approximately half that of the vessel's own natural roll frequency, though they may also occur at wave encounter frequencies that are multiples of half of the vessel's natural roll frequency.

2.2 (d) Impact Excitation

This mode of capsize occurs when a steep or breaking wave impacts the ship and results in an extreme roll angle.

2.2 (e) Large Amplitude Roll

This mode of capsize may be single or multiple rolls produced by other dynamic effects (e.g. broaching – following a large sudden yaw) in addition to wind and wave forces.

2.3 DYNAMIC RESPONSES CONTRIBUTING TO CAPSIZE

2.3 (a) Broaching

Broaching is a type of ship directional instability which is characterized by a sudden large yaw from the original heading. A broach can arise in following and stern-quartering seas and may manifest itself in a number of ways:

Successive Overtaking of Waves – This mode of broach occurs during the passage of several steep waves, gradually forcing the ship into beam seas. It occurs in steep following and quartering seas when the ship is travelling at a speed less than the mean wave group speed.

Low-Frequency, Large-Amplitude Yaw Motions – This typically happens at higher ship speeds in moderate stern-quartering seas. A gradual build-up of oscillations in yaw occurs as successive waves impinge on the ship from behind. As the motion hits resonance, yaw amplitude increases until large amplitude yaw motions are displayed.

Broaching Caused by a Single Wave – Usually the result of one or a number of motions that include surf riding or bow submergence and coupled pitch, roll and yaw instability at high speed. All are possible in following or stern-quartering seas.

2.3 (b) Surf Riding

Surf riding results from the ship moving down a wave crest with increasing speed. Large dynamic side forces may result if the ship imbeds itself in the proceeding wave. These dynamic forces may add to other dynamic forces to produce a dynamic capsize. Surf riding most frequently occurs when the ship is travelling near the wave speed.

2.4 HISTORY

In the eighteenth century, scientific investigation highlighted the importance of knowing the position of the ship's centre of gravity. A direct calculation method was initially applied to a few ships; however, the calculations were laborious and the accuracy was often in doubt.

The metacentric theory was published by Pierre Bouguer in 1746 (1). Its application was further advanced in the later half of the eighteenth century by the development of the inclining experiment. The first known inclining experiment, conducted in the UK, was that of the eighteen gun vessel *Scylla* in 1830.

Determining the position of the centre of gravity together with the application of the metacentric theory enabled the metacentric height (GM) to be determined in any loading condition. However, the significance of the GM calculation was not appreciated until the capsize of the steam ship *Perseverance* at Woolwich in 1855. This loss resulted in the first attempt to define a minimum GM criterion; however, its applicability was a subject of great debate.

The original formulation of the metacentric theory was constrained by small angle theory. In 1796 Atwood (2) published the now well known formula for determining the righting lever (GZ) at large angles of heel. However, it was not until 1876 that Messrs Barnaby and Barnes devised a way of applying Atwood's formula using radial integration.

¹ The phrase "wave encounter frequency" is the common-usage term for what is technically the wave group encounter frequency.

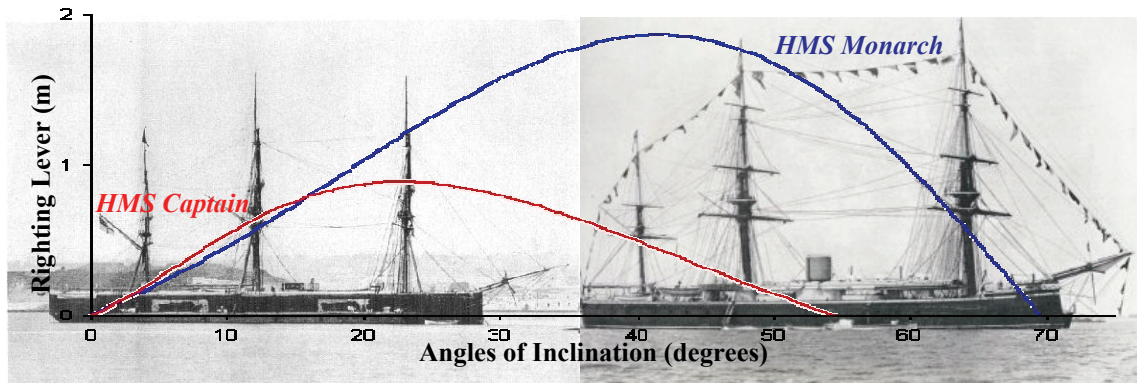


Figure 2. Comparison of righting arms, HMS Captain and HMS Monarch.

It was the capsizing of HMS *Captain* in 1870 that caused the significance of the GZ curve to be realised (3). HMS *Captain* was considered to have superior stability to similar vessels of the time by virtue of her larger GM. The *Captain* was lost in a storm while HMS *Monarch*, a ship with lower GM but higher maximum GZ and greater range of positive stability (see Figure 2), survived the same storm. After the loss of the *Captain*, the significance of the GZ curve as a further indication of ship stability, became generally accepted. It was this event that caused the safety of Royal Navy ships subsequently to become subject to formal certification. Criteria for GM and GZ were formulated, but not divulged.

With the end of the sail era, formal intact stability criteria were adopted. For example: GM greater than 1 foot; maximum GZ greater than 1 foot; angle of maximum GZ at least 30°; GZ at 30° and at 40° greater than 1 foot; and range of positive stability 70° or greater.

Damage stability criteria were, however, little more than positive stability when flooded to a specified extent.

In subsequent years, further research led to the stability criteria of many navies being updated. The most significant research was the comprehensive study undertaken by Sarchin and Goldberg in 1962 (4). This study proposed a standard set of empirically defined stability criteria for United States Navy ships based on detailed investigations of intact capsize of three US destroyers in a Pacific typhoon in 1944. It is the set of criteria developed in this 1962 study that form the basis for the majority of modern warship stability criteria applied by many nations. These criteria include consideration of the intact conditions of beam wind combined with rolling, lifting of heavy weights over the side, crowding of passengers to one side, high speed turning, and topside icing. Damage stability criteria were also proposed based on weapon effects and survivable damage lengths from World War II experiences.

Subsequently some national naval standards, originally based on Sarchin and Goldberg, have been modified and

supplemented with the addition of GZ shape criteria for small angles, 0° - 30°, 0° - 40° and 30° - 40°. These criteria are based on those proposed by Inter-Governmental Maritime Consultative Organization (now International Maritime Organization) in 1969 (5) which originated from the investigations and research of Rahola in 1939 (6).

These hydrostatics-based standards have attempted to incorporate some consideration of the dynamic issues, albeit 'quasi-statically', through the application of gust factors to wind heeling levers, the use of roll back angles (see Figure 3), and in some cases the consideration of the diminution of the righting arm when the ship is balanced on a wave (7 & 8).

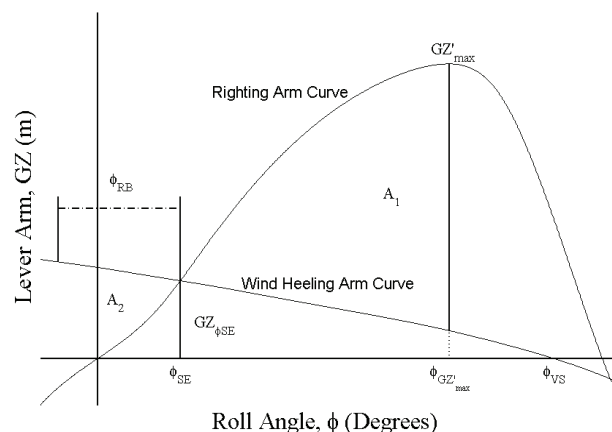


Figure 3. Typical GZ Curve with Wind Heeling Arm.

2.5 APPLICATION

It is known that the static stability criteria values include some margin to account for the relatively crude nature of the calculation methods employed at the time of their inception. It is significant to note that the exact rationale behind the determination of these factors and approximations are no longer clear. It is this lack of clarity in conjunction with the apparently good service provided by such standards over the last forty years that has resulted in an understandable uncertainty and hesitancy to question their application and validity.

This uncertainty has led to situations whereby full compliance to a standard is demanded by the stability authority, with extremely small short-falls against a single criterion considered unacceptable.

In contrast to the rigid application of these criteria is the broad range of vessels to which they are applied. With the exception of the applicable nominal wind speed used, it is not unusual to see the same set of intact stability criteria being rigorously applied to vessels ranging from harbour tugs to aircraft carriers. It is assumed that this broad brush application results from the lack of alternatives and the perception of good service rendered by that standard.

2.6 THE IMPACT OF MODERN SHIP DESIGNS

It is questionable if the types of vessels against which Sarchin and Goldberg (4) developed their criteria (two designs pre-dating WWII), exemplify their modern equivalents in terms of dynamic stability. However, for the reasons set out in the preceding section, standards such as Sarchin and Goldberg and its derivatives are still being applied.

Radical departures from conventional displacement designs are now becoming increasingly common. These include the application of 'tumble home', deep 'V' and wave-piercing bow forms, and the inclusion of more hull integrated watertight superstructure.

One of the most significant and common departures from those original forms is the change in aft body design, with notably wider transoms forms (see Figure 4). While these modern wide transoms forms are designed to satisfy Sarchin and Goldberg criteria, they can manifest significant dynamic stability characteristics that are not reflected in the criteria and are unlikely to have been so prevalent in the performance of the original forms. This change in aft body form has led to higher initial values of GM; a propensity for significant diminution of the static righting lever when the vessel is balanced on a steep wave (crest amidships); a susceptibility to dynamic roll excitation due to significant fluctuations in waterplane area inertia during the passage of steep overtaking waves; and a potential for broaching due to large Froude-Krylov forces induced by the waves on the more full aft body.

Moreover, there have been, at concept level, cases where more radical hulls have been developed and assessed as meeting the current 'quasi-static' stability criteria, but upon experimental assessment of their dynamic performance, they have been found to exhibit poor, if not catastrophic, dynamic stability characteristics. Commonly these are resolved by reducing the KG (significantly) and increasing the aft body flare. Such cases highlight the risk and potential limitations of employing traditional criteria to non-traditional forms

and the inability of the traditional criteria to fully capture these dynamic issues.

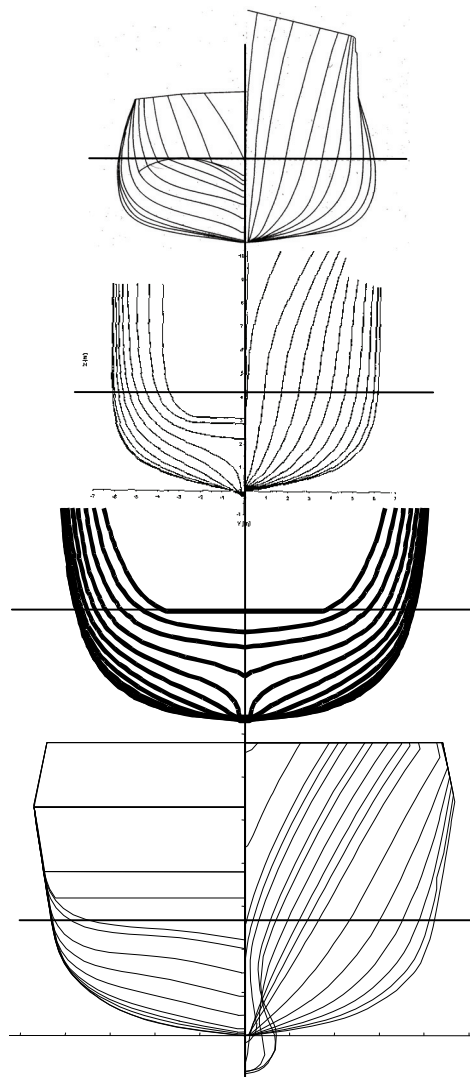


Figure 4 . Transition over time to wide transom forms.

Clearly the level of safety attained with modern hull forms is not necessarily the same as that which was intended for the criteria when they were derived. If the use of traditional static stability standards is to be continued then the following questions need to be addressed:

- What risk of capsize have we accepted through the application of current Sarchin and Goldberg based criteria?
- What are the limitations of applicability of current Sarchin and Goldberg based criteria with respect to hull form?
- How should the stability of modern vessels be assessed if the current criteria and 'quasi-static' approach are no longer applicable?

2.7 THROUGH-LIFE STABILITY MANAGEMENT

Due to the unknown implications of marginal non-compliances against a criterion, it is usual to demand total compliance. While this is easily achievable at the start of a warship's life, maintaining full compliance becomes increasingly difficult later in life due to increases in KG and displacement.

Eventually this 'growth' results in failure to meet one or a number of criteria, and consequently the placement of restrictions upon the vessel or class. Often, in order to maintain the minimum centre of gravity needed to comply with the standard, use of consumable fluids is limited. In more severe cases the wind speed and sea state in which the vessel is allowed to operate may also be reduced. Such restrictions are highly undesirable for naval combatants with a remit of rapid deployment to any area. To counteract the effects of 'growth', highly expensive ship life extension programs are occasionally required, which at best involve the costly fitting of solid ballast.

To facilitate a more balanced and cost-effective approach to through-life stability management, it is imperative to come to a clear understanding of the sensitivity of each criterion as an indicator of extreme dynamics and risk of capsize, i.e. how changes in the value of the criterion used in the standard affect the criterion's ability to indicate risk.

2.8 CHANGING PROCUREMENT

Increasingly, commercial standards are being adopted in place of defence standards, with the rationale being that they offer better value for money. This may indeed be true in many instances, provided the role and fitness for purpose of the commercial standards are fully compatible with the required naval capability.

Adopting a standard that has been developed to reflect a non-military role in a specific global environment and then operating the vessel outside those assumptions means the level of safety defined by the standard is no longer certain.

To discern the implications of adopting non-military standards for naval vessels, it is important to know both the sensitivity of criteria within the standard as extreme-motion indicators, and what level of safety is assured by compliance with the standard.

In summary, for both procurement and through-life management purposes, it is necessary to adopt logical and cost-effective processes for assessing dynamic stability, including adopting an appropriate stability standard, whether commercial or military. Practical and efficient use of the standard requires an understanding of

the level of safety inherent in the standard and of the sensitivity of that level of safety to changes in the values of the constituent criteria (both individually and jointly).

3. THE NAVAL SHIP STABILITY STANDARDS WORKING GROUP

The Co-operative Research Navies (CRNAV) Dynamic Stability group was established in 1989 to undertake research into the underlying physical phenomena and characteristics of dynamic stability. The work has led to the development and application of suitable dynamic stability simulation tools in pursuit of this objective. In light of the significant advances made by the group, the concerns with current stability standards could now be investigated in more detail.

Since the responsibility for naval stability standards rests with the naval organisations, it was considered appropriate to form a new group lead by the navies. The Naval Stability Standards Working Group (NSSWG) was formed in 1999 from the naval members of the CRNAV group, as follows:

- Department of Defence (Australia).
- Department of National Defence (Canada).
- Ministère de la Défense (France).
- Ministerie van Defensie (Netherlands).
- Ministry of Defence (UK).
- United States Coast Guard (USA).
- Naval Sea Systems Command (USA).

The naval members are supported by the following guest members from their associated research organisations:

- Australian Maritime College.
- Defence Research and Development Canada.
- Bassin d'Essais des Carènes (France).
- Maritime Research Institute (Netherlands).
- QinetiQ (UK).
- Naval Surface Warfare Center (USA).

The objective of the group is '*To develop a shared view on the future of naval stability assessment and develop a Naval Stability Standard Guidelines document which can be utilised by the participating navies at their discretion.*'

At a practical level, this involves identification of methods of relating stability criteria to risk. In the short-term, this means identification of level of safety extant in the current standards, focusing on the strengths and weaknesses of existing standards, and using a standard set of environmental conditions. In the long term, it means developing methodologies for assessing stability characteristics and practical limits for both design and life-cycle management.

4. APPROACH

Figure 5 maps the process adopted. The objective is best achieved by an approach that initially concentrates on investigating the level of safety associated with current standards. Resolving this issue would support the development of guidance on the ability of current standards to reflect dynamic stability, the determination of their applicability with respect to modern forms, and the establishment of suitable alternative approaches for assessment.

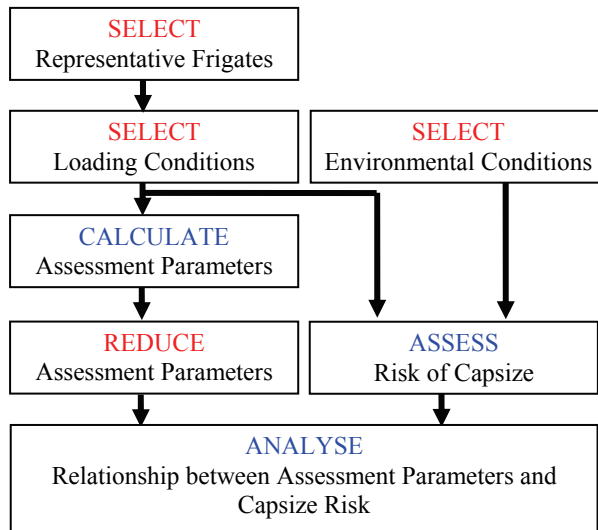


Figure 5 . Schematic view of approach adopted.

4.1 THE PROBABILISTIC METHODOLOGY

In order to investigate the efficacy of existing 'quasi-static' intact stability standards a methodology was required to determine the probability of capsizing. The technique adopted considers the full gamut of credible combined wave and wind climates possible in the lifetime of such a vessel and its physical behaviour in the various sea states. As such it includes consideration of those extreme conditions that, although having a small probability of occurrence, may well be critical to safe operation.

The probability of capsizing is assumed to be directly related to the probability of exceeding a critical roll angle: $P(\phi > \phi_{critical})$. The methodology employed in determining the probability of exceeding a critical roll angle in a particular loading condition is that described by McTaggart (9, 10).

The method combines time domain simulations from the ship motion program FREDYN (11) with probabilistic input data for the wave conditions and heading and speed of the ship via a two-step process called PCAP. The first step is the program Pcapref, which computes the maximum roll angles from the FREDYN simulations. The second step is the program Pcapsize2, which combines the Pcapref results with the other statistical

data to determine the probability of capsizing (or of exceeding a critical roll angle, whether capsizing actually occurs or not). The probability of exceeding the critical roll angle in a given duration (D) is given by:

$$P(\phi > \phi_{critical}) = \sum \sum \sum \sum p(V) p(\beta) p(H_s, T_p) \times P(\phi > \phi_{critical} | V, \beta, H_s, T_p) \quad (1)$$

where V is the vessel's speed, β is the vessel's heading, H_s is the significant wave height, T_p is the peak wave period, and their joint probability density is $p(H_s, T_p)$. Each independent variable (X) is discretised into N_X different values. The final probability term, $P(\phi > \phi_{critical} | V, \beta, H_s, T_p)$, is the conditional probability of exceeding the critical roll angle given a specific combination of speed, heading, and seaway conditions. This term is determined by finding the probability of exceedance for maximum roll angles from multiple FREDYN numerical simulations using a fitted distribution or a distribution-free probability method.

The required calculations for a single vessel-loading condition combination can take up to 20 CPU days (based on 3 speeds, 13 headings, 20 wave heights and 15 periods). Since this study involves 12 vessels, each having a minimum of 9 applicable loading conditions a cluster of 12 PCs was used in an attempt to reduce computational time involved. The strip theory based computations took approximately 100 days using the cluster.

4.2 ASSUMED CONDITIONS

4.2 (a) Operational Conditions

There are two basic operational probability distributions assumed in determining the capsizing probability, in addition to the input environmental probability distribution which is discussed later. The first, $P(V)$, is a discretised distribution for three calm water speeds derived from a representative naval frigate operational speed profile. The second is $P(\beta)$, a uniform distribution of headings.

It is important to note that these operating distributions are independent of any operator action; there are no voluntary or involuntary heading related speed reductions. Therefore the probability of exceeding the critical roll angle determined should be considered a baseline and reflects only the influence of the 'quasi-static' stability standards and hull form characteristics, and not the added influence of the good seamanship of the operator.

4.2 (b) Environmental Conditions

Intact capsizing is clearly related to encountering a critical environment in a manner such that one or a number of capsizing mechanisms are invoked. The probability of

exceeding the critical roll angle is therefore related to the probability of occurrence of a given environment (see Equation (1)). For the purposes of this study the Bales North Atlantic scattergram (12) was modified slightly (9, 10) and used to define the probability distribution of uni-directional seas conforming to the Bretschneider Spectrum.

Since the wind conditions are typically related to the wave conditions, an approximation was employed that assumed that winds were not only co-directional with waves but linearly related to the significant wave height (9, 10).

4.3 THE FRIGATES

Careful consideration was given to the selection of vessels for this investigation, as the selected set of ships must allow:

- The exposure of the probability of capsize currently accepted through the application of standards based on Sarchin and Goldberg,
- the change of capsize risk associated with the recent evolution of the frigate form,
- the ability of particular GZ assessment parameters to reflect the dynamic stability performance.

The working group selected a total of twelve frigates representing all participant navies. Each vessel is of a class that is either currently in service or that has seen significant periods of service. The designs can be considered to span at least the last 40 years. Some of the designs predate the inception of the Sarchin and Goldberg criteria, but were required to meet them later in life. The majority of the vessels were designed from the outset to meet either Sarchin and Goldberg or derivatives of that standard. Table 1 shows the range of basic form parameters of the selected frigates.

Table 1. Range of Basic form Parameters.

Parameter:	Min	Max
Displacement (tonnes) - Δ	2478	5490
Length at Waterline (m) - L	106.68	124.50
Beam at Waterline (m) - B	12.19	15.23
Draft (m) - T	3.81	5.33
Depth (m) - H	8.89	11.69
Vertical. CG (m) - KG	5.00	7.20
Metacentric Height (m) - GM	0.250	1.649
$CB = \Delta / (L * B * T)$	0.440	0.548
$CWL = AWL / (L * B)$	0.718	0.810
$CVP = CB / CWL$	0.593	0.698
L/B	7.873	9.160
KG/H	0.539	0.738
KG/B	0.404	0.497
KG/T	1.120	1.671
GM/B	0.020	0.121
AWL: Waterplane area		

Each navy selected a matrix (3 displacements x 3 KGs) of loading conditions for their vessels. These loading conditions were determined with the benefit of practical knowledge and experience of the particular class involved.

In order to ensure the multiple objectives were accomplished, the matrix bounded actual operating load conditions, whether they were driven by intact stability considerations or those of damage stability (see Figure 6). The matrix was intended to encompass sufficient conditions so as to allow future consideration of damage stability to be viewed in light of its impact upon intact capsize risk. The outer boundaries of the matrix were required to include combinations of KG and displacement that would fail a number of criteria in order to expose their associated probability of capsize.

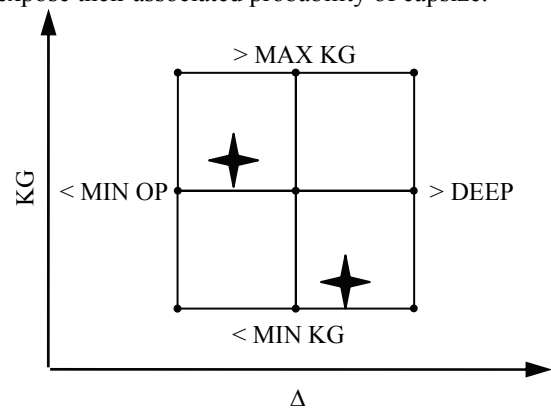


Figure 6 . The Conceptual Matrix of Loading Conditions.

4.4 GZ PARAMETERS

A set of 'quasi-static' measures that represent the majority of those used to evaluate stability performance in the various naval and commercial standards was assessed. The measured (simulated) parameters rather than specific criteria values were examined in order to allow the following:

- Investigation of the ability of particular measures to reflect dynamic stability.
- The probability of exceeding the critical roll angle associated with a number of different standards to be determined.
- Exposure of the criteria values needed to achieve a specific probability of exceeding the critical roll angle.

The selected GZ assessment parameters can be considered, or categorised, by the degree by which the dynamic environment is considered.

4.4 (a) Fully Static

At the most basic level are the fully static measures whereby the shape and area characteristics of the calm

water righting curve are assessed. The basic shape parameters selected are given in Table 2 and Figure 7.

Table 2 . Fully Static Shape Parameters.

Parameter	Description
GM	The metacentric height (fluid) (metres).
ϕ_{GZmax}	The angle at which the maximum righting lever arm occurs (degrees).
RPS	Range of positive stability (degrees).
GZ_{max}	The maximum righting lever arm (metres).
GZ_{30°	The righting lever arm at 30° (metres).

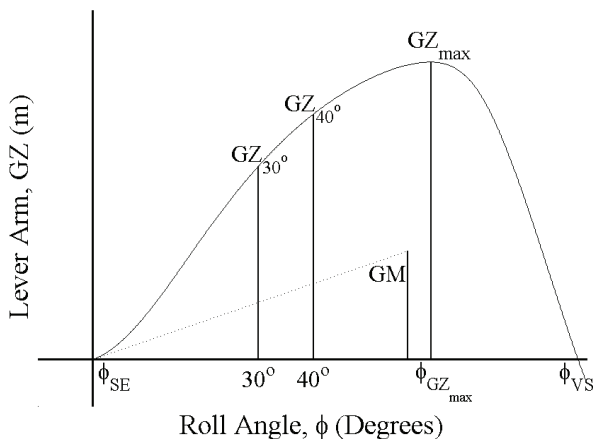


Figure 7 . Fully Static Shape Parameters.

For the most part, these parameters significantly predate Sarchin and Goldberg. As such they have been applied by some naval organisations for a very significant period of time and can be considered to be the framework upon which such standards as the UK Royal Navy's DEFSTAN 02-109 (13) were built.

The basic GZ area characteristics selected are given in Table 3 and Figure 7. These parameters are based on those proposed by International Maritime Organisation (IMO) in 1969 (5), and originate from the research of Rahola in 1939 (6). These measures were added to the UK navy standard (13), though with enhanced criteria, and have subsequently been adopted by other navies.

Table 3 . Fully Static Area Characteristic.

Parameter	Description
$A_{0^\circ-30^\circ}$	The area under the GZ curve between 0° and 30° . (m-rads)
$A_{0^\circ-40^\circ}$	The area under the GZ curve between 0° and 40° . (m-rads)
$A_{30^\circ-40^\circ}$	The area under the GZ curve between 30° and 40° . (m-rads)

A further set of fully static assessment parameters is also included (see Table 4). These were derived by the CRN group (14) and although they are clearly fully static in their form, the underlying associated criteria were

determined through an extensive series of FREDYN simulations of the dynamic behaviour of 30 frigate-type hull forms in a given set of idealised, critical, environmental conditions.

Table 4 . Further Parameters.

Parameter	Description
$A_{\phi_{SE}-\phi_{VS}}$	Total (dynamic stability) area under the GZ curve. (m rads)
CVP	Vertical prismatic coefficient

4.4 (b) Energy Balance

The next set of terms considered were those which apply an "energy balance" approach. These assess the relationship between the shape and area characteristics of the calm water righting curve with respect to an induced wind heeling curve (see Table 5 and Figure 8). These are the Sarchin and Goldberg measures that relate to the relationship between the wind heeling arm and righting arm. It is this set of criteria that has formed the basis, or core, of the majority of current naval stability standards. In the original Sarchin and Goldberg (4) criteria and therefore the US Navy standard (DDS 079-1) (15), these parameters are related to the application of a 100 knot beam wind heeling lever.

Table 5 . Energy Balance Parameters.

Parameter	Description
ϕ_{SE}	The angle of the intersection of the wind heeling lever with the GZ curve. (degrees)
$\frac{GZ_{\phi_{SE}}}{GZ_{max}}$	The ratio of GZ at ϕ_{SE} to the maximum GZ.
A_1	The area between the GZ curve and the wind heeling lever between ϕ_{SE} and the down flooding angle, ϕ_{DF} . (m rads)
A_2	The area between the GZ curve and the wind heeling lever between ϕ_{SE} and a roll back angle, ϕ_{RB} , of 25° . (m rads)
A_1 / A_2	The ratio of the A_1 and A_2

4.4 (c) Wave Adjusted

The final set of parameters are those that, in place of the calm water righting curve, employ a righting curve determined from the vessel being balanced in the trough and or on the crest of a wave of height and length proportional to the vessel length.

$$H = \frac{\lambda}{10 + 0.05\lambda} \quad (\text{m}) \quad (2)$$

where the wavelength, λ , is equal to the waterline length of the vessel.

Figure 8 . Energy Balance Parameters .²

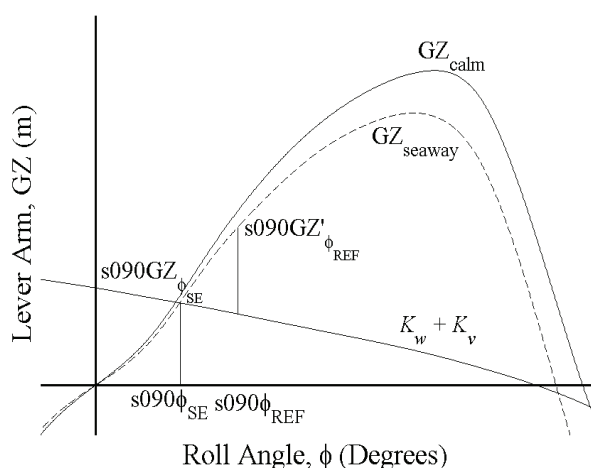
In addition to balancing in a trough and on a crest, GZ curves were developed for what is termed the ‘seaway’ righting arm, the mean of the crest and trough curves:

$$GZ_{seaway} = \frac{GZ_{trough} + GZ_{crest}}{2} \quad (3)$$

Table 6 and Figure 9 illustrate the wave-adjusted GZ parameters selected. These GZ parameters are related to those embodied in van Harpen (7) (the RNIN standard). Such standards also tend to apply energy balance assessments.

Table 6 . Wave Adjusted Parameters.

Parameter	Description
$GZ'_{\phi_{REF}}$	The residual righting lever arm at ϕ_{REF} with a beam wind.
$RRPS$	The residual range of positive stability.
$A'_{\phi_{SE}-\phi_{VS}}$	The residual area under the GZ curve, above the wind heeling lever arm curve, and above the $GZ = 0$ axis.

Figure 9 . Wave Adjusted Parameters.³

² In this figure, n100 refers to no wave balancing (or nominal GZ curve) with a 100 knot wind heeling lever arm applied.

A full listing of all the GZ assessment parameters is given in Table 13 of the Appendix.

4.4 (d) Form Parameters

A number of hull form parameters were also selected for inclusion in the analysis in order to allow the differentiation between traditional and more modern forms (see Section 2.6). These include basic particulars like displacement, form coefficients like the block coefficient, and characteristic ratios such as length to beam. A full list is given in Table 15 of the Appendix.

4.5 ASSESSMENT OF ‘QUASI-STATIC’ PERFORMANCE

An assessment of those parameters detailed in section 4.4 was undertaken for each ship/loading condition. It is to be noted that all analyses undertaken assume that superstructure is included with respect to the determination of the wind heeling lever only. The superstructure was excluded from buoyancy calculations since it was considered that its inclusion would obfuscate the important issues of hull geometry.

The outputs from PCAP Analysis and FREDYN, along with some additional information, are post-processed using MATLAB.

For each ship, the probability of exceeding the critical roll angle within one hour can be broken down by significant wave height (upper left plot in Figure 10), wave period, (the upper right plot in Figure 10), or by ship speed and heading (lower plot in Figure 10). This allows for the identification of significant risk under specific conditions. The probabilities conditional on wave height and wave period can be plotted over the scattergram (see Figure 11, where the numbers represent percent probability of that condition occurring, but for the sake of the plot they only provide a visual clue as to which seaways are realistic as opposed to those that would involve waves too steep to sustain their form). Polar plots can also be developed from the data broken down into speed-heading combinations. See Figure 12 for example polar plots of the conditional capsize probability for all possible (H_s, T_p) , where the top plot shows a surface plot of the risk (i.e., the “big picture”), while the bottom plot shows the same information as contours of risk (details).

³ In this figure, s090 refers to a ‘seaway-balanced’ GZ curve with a 90 knot wind heeling lever arm applied. Other GZ ‘balancing’ and wind speeds were also examined.

Figure 10 . Top Left: $P(\phi > \phi_{\text{critical}})$ in one hour by Significant Wave Height; Top Right: $P(\phi > \phi_{\text{critical}})$ in one hour by Peak Wave Period; Bottom: $P(\phi > \phi_{\text{critical}})$ in one hour by Speed and Heading.

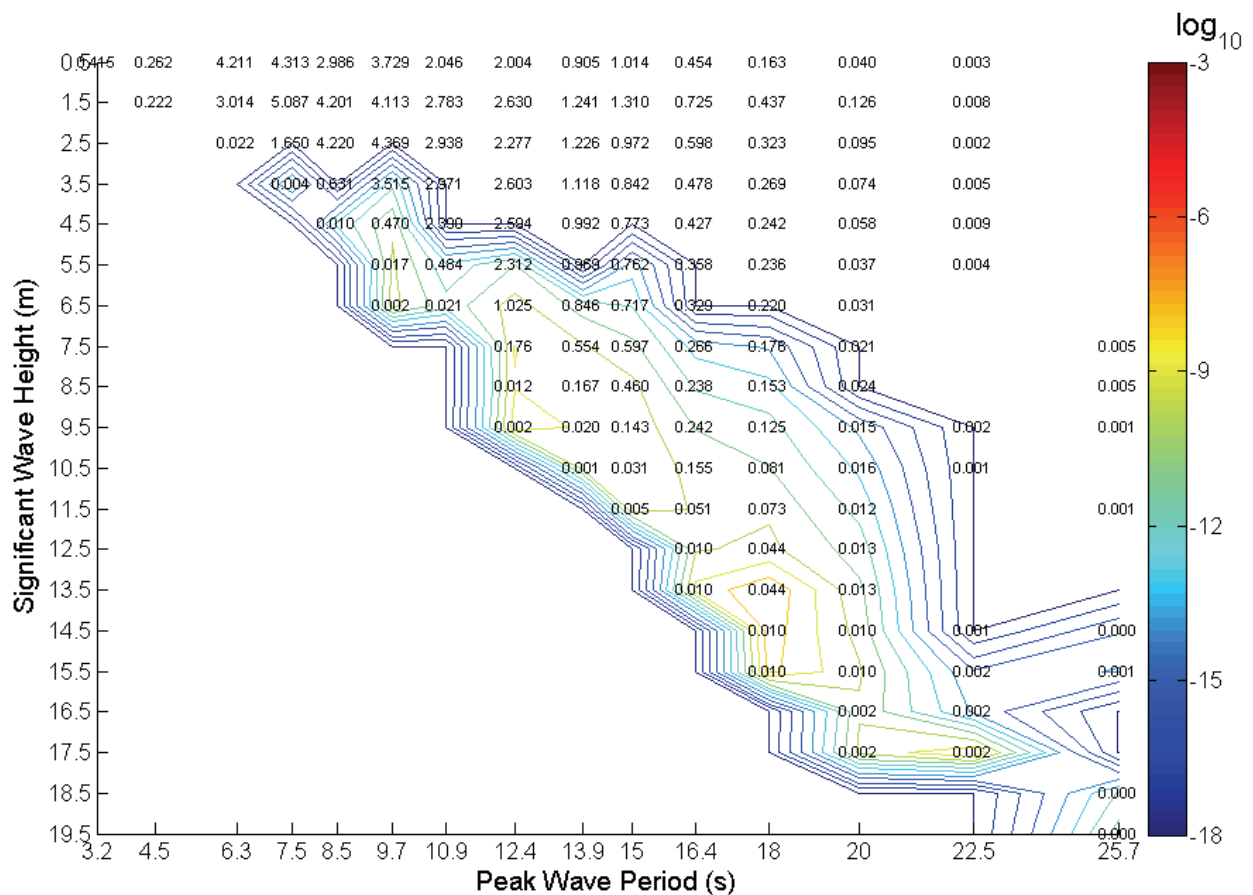


Figure 11 . $P(\phi > \phi_{\text{critical}} | H_s, T_p)$ vs H_s, T_p for all Speeds and Headings, 1 Hour Exposure.

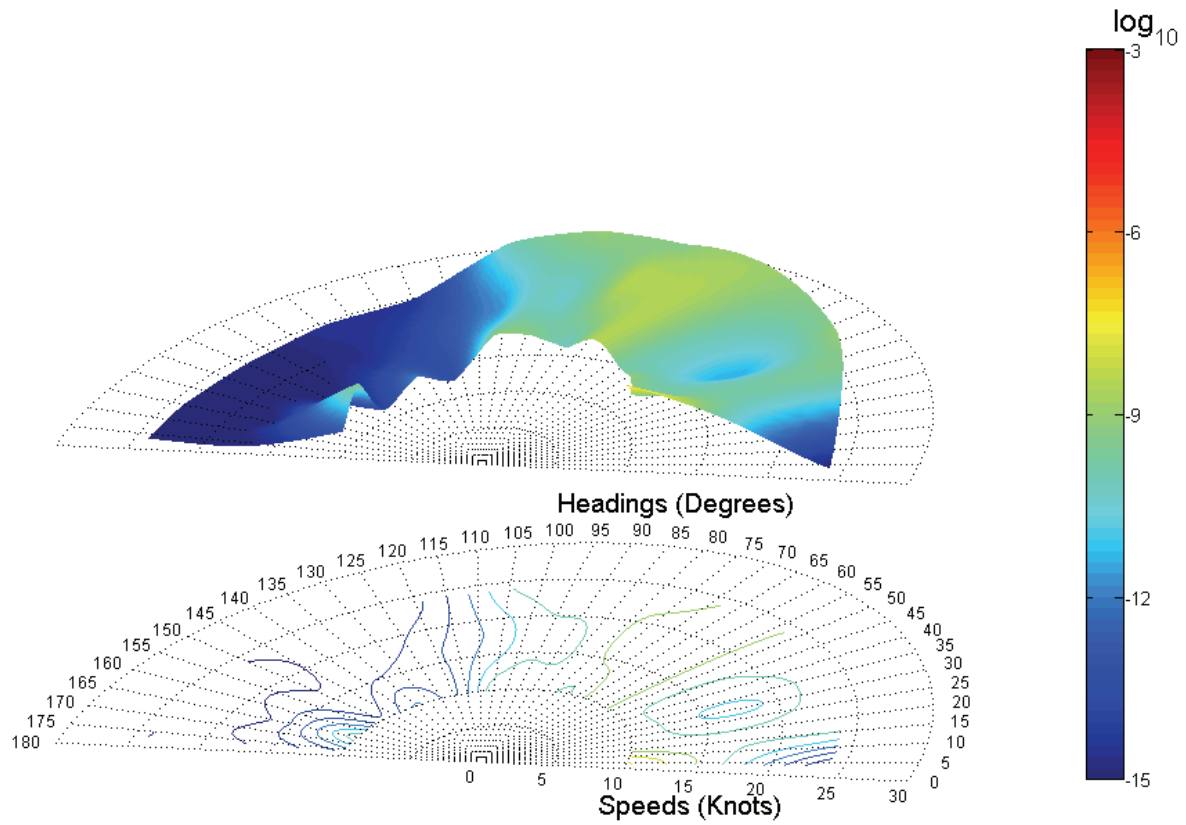


Figure 12. Polar-Contour Plot of $P(\phi > \phi_{\text{critical}} | V_s, \beta)$ vs V_s, β for all Sea States.

Figure 13. Top Left: $P(H_s | \phi > \phi_{\text{critical}})$ in one hour by Significant Wave Height; Top Right: $P(T_p | \phi > \phi_{\text{critical}})$ in one hour by Peak Wave Period; Bottom: $P(H_s/\lambda | \phi > \phi_{\text{critical}})$ by Steepness (H_s/λ).

Figure 14 . Left: $P(V|\phi > \phi_{critical})$ vs V by sea state; Right: $P(\beta|\phi > \phi_{critical})$ vs Heading by sea state.

Additionally, an approach was employed that determined those speeds, headings, and wave parameters that were associated with highest (hourly) conditional probability given capsizing using variations of the formulation given in (4).

$$P(V, \beta, H_S, T_P | \phi > \phi_{critical}) = \frac{P(V)P(\beta)P(H_S, T_P) \times P(\phi > \phi_{critical} | V, \beta, H_S, T_P)}{P(\phi > \phi_{critical})} \quad (4)$$

These conditional probabilities are also produced by the MATLAB post-processing in the form of a series of histograms showing their distribution for each ship in order that additional insight may be gained into the underlying phenomena. For example, the upper left plot in Figure 13 addresses the question: If the critical roll angle is exceeded, what is the most likely significant wave height associated with the event? The upper right plot show the same information for wave period, while the lower plot examines wave steepness.

4.5 (a) Conditional Probabilities

The probabilities of exceeding the critical roll angle within one hour, given a specific sea state were also calculated.

$$P(\phi > \phi_{critical} | 0 < SS \leq A) = \frac{\sum \sum P(V)P(\beta) \times P(\phi > \phi_{critical} | V, \beta, H_S, T_P)}{\sum \sum P(V)P(\beta)} \quad (5)$$

where A represents the grouped (H_S, T_P) combinations associated with sea state definitions from ≤ 5 to "All" (the maximum encompassing the complete scattergram). The NATO sea state definitions (16) are used with the selected (North Atlantic) scattergram (12). These probabilities can be further delineated by ship speed or heading, allowing the identification of significant speed-seaway interactions (left plot in Figure 14) or heading-seaway interactions (right plot in Figure 14).

5. ANALYSIS OF RELATIONSHIP BETWEEN 'QUASI-STATIC' AND RISK RESULTS

A total of 124 ship/loading conditions representing 12 ships were processed in the manner set out in this document. A comprehensive statistical regression analysis was undertaken, the objective of which is to allow the determination of the ability and sensitivity of particular measures to reflect dynamic stability, as well as the ability and sensitivity of combinations of measures to reflect dynamic stability.

Figure 15 shows an idealisation of the basic concept of relating the probability (risk) to ship-related parameters. It shows the level of risk currently accepted through use of a particular criterion, and how the risk differs from ship to ship.

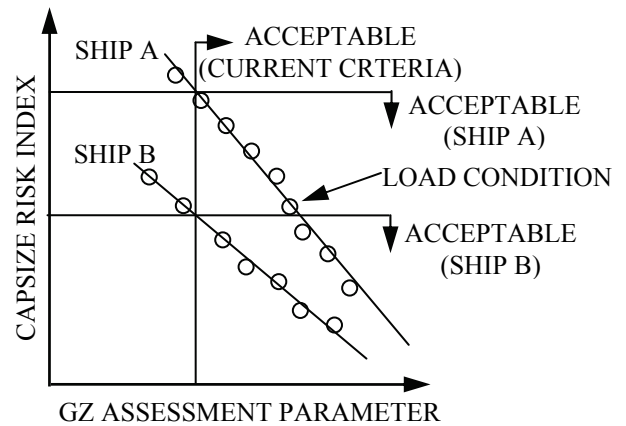


Figure 15. Idealisation of Probability of Exceeding the Critical Roll Angle vs GZ Assessment Parameter.

Figure 16 presents typical results for the 12 ships included in this study. The results show considerable nonlinear scatter. Figure 17 shows the same results with the probabilities on a log scale; the scatter is still significant and nonlinear.

broad indication of risk of capsize, and in some cases may even be outside the bounds of proper and normal operation of the ship.

There has been some debate over the probability values determined in the PCAP analysis. It is generally felt that the PCAP method overpredicts capsize in the long term (e.g., one year). Although the issue is primarily apparent in the long-term probabilities, the debate has fostered a desire to look at alternative probability methods. It has also lowered the confidence in the current probability values.

The assumptions inherent in the strip theory in FREDYN 8.2 may cause inaccuracies in some of the simulation results, also affecting the probability results.

Taken together, this means that the regression analysis results cannot be taken to be numerically accurate, and thus the relative strengths and weaknesses of GZ parameters for indicating risk of exceeding the critical roll angle are not strictly valid. The methodology, however, is a reasonable process.

Given the uncertainty in the accuracy of the results, it may be prejudicial to publish the actual numerical results. However, a qualitative sense of the trends may be shown via a colour mapping scheme. Each parameter of interest was regressed against the probability of exceeding the critical roll angle for a number of observations (loading conditions). The classic R^2 value is used as a measure of 'fit'; i.e., an R^2 value near 1 indicates the parameter can be used to indicate extreme motion. In Table 7 through Table 12, the shading indicates the quality of indication as follows:

$R^2 < 0.50$
 $0.50 \leq R^2 < 0.80$
 $0.80 \leq R^2 < 0.95$
 $0.95 \leq R^2 < 0.99$
 $0.99 \leq R^2$



It must be remembered that as the issues outlined above are dealt with, the colour maps may (or may not) change.

Figure 16. Typical Scatter of Probability Results - Linear Probability Scale

Figure 17. Typical Scatter of Probability Results – Log Probability Scale

6. DISCUSSIONS AND CONCLUSIONS

The primary purpose of the work to date has been to investigate the strengths and weaknesses of quasi-static measures and to expose their ability to reflect dynamic stability and ultimately the capsize risk.

6.1 CAVEATS

Loading conditions used in the present study do not necessarily reflect real working conditions for the ships involved. The loading conditions are intended to give

Table 7. Ship-by-Ship Correlation between Fully Static Shape Parameters and Probability of Exceeding the Critical Roll Angle (Ref Table 2 Figure 7).

	Ship 1	Ship 2	Ship 3	Ship 4	Ship 5	Ship 6	Ship 7	Ship 8	Ship 9	Ship 10	Ship 11	Ship 12
GM	Yellow	Yellow	Yellow	Yellow	Orange	Orange	Orange	Orange	Yellow	Yellow	Orange	Orange
ϕ_{GZmax}	Yellow	Red	Yellow	Yellow	Orange	Red	Yellow	Orange	Yellow	Orange	Red	Red
RPS	Yellow	Yellow	Yellow	Yellow	Orange	Red	Yellow	Orange	Yellow	Light Green	Orange	Orange
GZ_{max}	Orange	Yellow	Yellow	Yellow	Orange	Yellow	Orange	Orange	Yellow	Yellow	Orange	Orange
GZ_{30°	Orange	Orange	Yellow	Yellow	Orange	Yellow	Red	Red	Yellow	Yellow	Red	Orange

Table 8. Ship-by-Ship Correlation between Fully Static Area Parameters and Probability of Exceeding the Critical Roll Angle (Ref Table 3 Figure 7).

	Ship 1	Ship 2	Ship 3	Ship 4	Ship 5	Ship 6	Ship 7	Ship 8	Ship 9	Ship 10	Ship 11	Ship 12
$A_{\phi_{SE}-30^\circ}$												
$A_{30^\circ-40^\circ}$												
$A_{\phi_{SE}-40^\circ}$												

Table 9. Ship-by-Ship Correlation between Energy Balance Parameters and Probability of Exceeding the Critical Roll Angle (Ref Table 5 Figure 8).

	Ship 1	Ship 2	Ship 3	Ship 4	Ship 5	Ship 6	Ship 7	Ship 8	Ship 9	Ship 10	Ship 11	Ship 12
ϕ_{SE}												
$GZ_{\phi_{SE}} / GZ_{max}$												
A_1												
A_2												
$\frac{A_1}{A_2}$												

Table 10. Ship-by-Ship Correlation between Wave Adjusted Parameters and Probability of Exceeding the Critical Roll Angle (Ref Table 6 Figure 9).

	Ship 1	Ship 2	Ship 3	Ship 4	Ship 5	Ship 6	Ship 7	Ship 8	Ship 9	Ship 10	Ship 11	Ship 12
n050GZ' $_{\phi_{REF}}$												
n070GZ' $_{\phi_{REF}}$												
n090GZ' $_{\phi_{REF}}$												
s050GZ' $_{\phi_{REF}}$												
s070GZ' $_{\phi_{REF}}$												
s090GZ' $_{\phi_{REF}}$												
c050RRPS												
c070RRPS												
c090RRPS												
c100RRPS												

Table 11. Ship-by-Ship Correlation between Parameters Provided by CRN Study and Probability of Exceeding the Critical Roll Angle (Ref Table 4)

	Ship 1	Ship 2	Ship 3	Ship 4	Ship 5	Ship 6	Ship 7	Ship 8	Ship 9	Ship 10	Ship 11	Ship 12
$A_{\phi_{SE}-\phi_{VS}}$												

Table 12. Results by Sea State for Correlation between Pooled Fully Static Shape Parameters and Probability of Exceeding the Critical Roll Angle (Ref Table 2 Figure 7).

Sea States	≤ 7	≤ 8	All	SQ
GM				
ϕ_{GZmax}				
RPS				
GZ_{max}				
GZ_{30°				

SQ – All Sea States, Stern-Quartering Seas: $\beta = 0^\circ \rightarrow 45^\circ$

6.2 FINDINGS

The parameters associated with current stability standards (Table 7 through Table 11) show mixed results in terms of explaining the variation in the probability of exceeding the critical roll angle. The results of this study indicate reasonable relationships, in many instances, between risk of exceeding the critical angle and those GZ parameters that are employed in current naval standards. This tends to validate the use of these parameters for assessment of stability for a particular ship. The variation between ships, however, would indicate that few, if any, of the parameters can be used across all ships.

The study has shown that, on an individual parameter basis, many naval standards employ criteria, or measures, that may be redundant due to correlation with other parameters (e.g., see Table 8, where the colour pattern suggests that for each ship all the parameters have the same ability for indicating extreme motion). Additionally, although many parameters from the standards show correlation with the probability of exceeding the critical roll angle, there are other parameters, not currently part of the standards examined, that have higher correlation.

The van Harpen criteria (wave balanced GZ curves, see Table 10) tended to provide stronger results than the nominal (no wave balancing) GZ curve parameters.

It should also be noted that the form parameters provide less explanation of the variation in the probability of exceeding the critical roll angle. This may be because risk of capsizing is related to geometry and inertial properties of the ship, and the latter are not reflected in the form parameters.

When the ships are considered as a group, none of the standard parameters have a strong correlation with the probability of exceeding the critical roll angle (see Table 12). This may, however, be due to the simple approach of pooling the individual ship results, which may not be the best method.

A more sophisticated approach would be to make a closer examination of the results from individual ships, looking for common features. Forcing the regression models by choosing appropriate parameters based on results from all ships may lead to regression models that are common for all ships.

The results of this investigation will support the development of guidance on the ability of current measures of stability to truly reflect dynamic stability, especially with respect to modern hull forms. It will also enable the development of suitable alternative approaches for assessment of dynamic stability.

7. RECOMMENDATIONS

More analysis must be undertaken initially on a ship by ship basis in order that the following can be discerned:

- What probability of capsizing have we accepted through the application of current Sarchin and Goldberg based criteria? Does the application of the current criteria unduly influence the risk of capsizing?
- Does the application of current criteria to the modern form result in a risk of capsizing that differs to the original intended? What are the limitations of applicability of current Sarchin and Goldberg based criteria with respect to hull form?
- How should the stability of such vessels be assessed if the current criteria and 'quasi-static' approach is no longer applicable?

Capsizing risks determined on the basis of FREDYN version 8.2 simulations should be used in a relative manner only for assessing the relevance of particular parameters for indicating the dynamic stability of a ship. Absolute values of capsizing risks are likely to be inaccurate due to limitations in FREDYN 8.2.

Exposure of the criteria values needed to achieve a specific probability of capsizing needs to be addressed in the near future. It is not directly answered in this work

due to the known inaccuracies of the predicted capsize probabilities.

7.1 INVESTIGATION OF CURRENTLY ACCEPTED CAPSIZE RISK

Investigating the currently accepted level of risk should use a FREDYN version 9.8 or higher where the approach based on the long wave assumption is replaced by a three-dimensional panel methodology for the determination of the Froude-Krylov forces. Furthermore, the panel method for determining the wave radiation and diffraction forces should be used, to give more accurate predictions at large heel angles.

The loading conditions selected must expose the level of safety currently accepted through the application of the standards. To this end a selected number of the original ship set are to be chosen for further simulations with their actual operational minimum and maximum loading conditions and an intermediate 50% condition. In order to truly reflect accepted levels of capsize risk, the load cases should be those used in practice, whether driven by intact or by damage stability.

Investigations of new methods for assessing the dynamic stability of vessels can only be evaluated after coming to an understanding of what is accomplished through use of the current standards. At that point, the results of the current and follow-on studies will inform the development of new procedures.

REFERENCES

1. Bouguer, P. 'Traité du Navire', Jombert, Paris, 1746.
2. Attwood, E.L., Pengelly, H.S., Sims, A.J., 'Theoretical Naval Architecture', Longmans, Green and Co, 1953 edition, originally published 1899.
3. Anonymous, 'The Stability of the *Captain, Monarch*, and other Iron-Clads', Naval Science, volume 1, (E.J. Reed, ed.), 1872.
4. Sarchin, T. H., and Goldberg, L. L., 'Stability and Buoyancy Criteria for U.S. Naval Surface Ships', SNAME Transactions, New York, Vol. 70, 1962.
5. A.167(ES.IV), 'Recommendation on intact stability for passenger and cargo ships under 100 metres in length', IMCO, 1969, Superseded by A.749(18), Amended by A.206(VII).
6. Rahola, 'The Judging of the Stability of Ships and the determination of the Minimum Amount of Stability Especially Considering the Vessel Navigating Finnish Waters', PhD Thesis, Technical University of Finland, Helsinki, 1939.
7. van Harpen, N.T., 'Eisen te stellen aan de stabiliteit en het reserve-drijfvermogen van bovenwaterschepen der Koninklijke Marine en het Loodswezen', April 1970.
8. BV1033, Bauvorschrift für Schiffe Bundeswehr - Marine. '1033 Stabilität der Überwasserschiffe', Bundesministerium der Verteidigung. German Federal Navy.
9. McTaggart, K.A., 'Capsize Risk Assessment Using Fredyn Ship Motion Predictions', Defence Research Establishment Atlantic. Canada, (DREA TM 99/149), 1999.
10. McTaggart, K.A., De Kat, J. O., 'Capsize Risk of Intact Frigates in Irregular Seas', SNAME Transactions, 2000.
11. De Kat, J. O., Brouwer, R., McTaggart, K.A., and Thomas, W.L., 'Intact Ship Survivability in Extreme Waves: New Criteria from a Research and Naval Perspective'. Fifth International Conference on Stability of Ships and Ocean Vehicles, STAB '94 Conference, Melbourne, Florida, Nov. 1994.
12. Bales, S.L., Lee, W.T., and Voelker, J.M., 'Standardized Wave and Wind Environments for NATO Operational Areas'. David Taylor Naval Ships Research and Development Center. (Report DTNSRDC/SPD-0919-01), 1981.
13. Naval Engineering Standard N.E.S. 109 Part 1 Issue 4, 'Stability Standards for Surface Ships Part 1, Conventional Ships', U.K. Ministry of Defence, 1999.
14. 'Naval Stability Standards Working Group Bridge Simulator Workshop "Operator Risk Mitigation – Extreme Weather Conditions"', Naval College & DMKM/Martech, Royal Netherlands Navy., 13–15 March, 2002.
15. Naval Ship Engineering Centre, 'Design Data Sheet – Stability and Buoyancy of U.S. Naval Surface Ships', DDS 079-1, U.S. Navy, Naval Sea Systems Command, Washington DC, 1 August 1975.
16. 'Standardized Wave and Wind Environments and Shipboard Reporting of Sea Conditions', STANAG 4194, edition 1, North Atlantic Treaty Organization (NATO), 6 April 1983.

APPENDIX

PARAMETERS USED IN ANALYSIS

Table 13. Stability Assessment Parameters from GZ Curve

Parameter	Description	Reference
GM	The metacentric height (fluid) for the ship at the given loading condition.	Bouger
ϕ_{SE}	The angle of static equilibrium for the ship at the given loading condition. This angle is typically, but not necessarily, 0° . With a beam wind it is the angle at which the wind heeling lever arm curve first intersects the GZ curve.	RN c. 1900 Sarchin (4)
ϕ_{VS}	The angle of vanishing stability for the ship at the given loading condition, with or without a wind.	
ϕ_{GZmax}	The angle at which the maximum righting lever arm occurs for the ship at the given loading condition.	RN c. 1900
$\phi_{GZ'max}$	The angle at which the maximum residual righting lever arm occurs for the ship at the given loading condition, with a beam wind of W knots.	
ϕ_{REF}	The reference angle for the ship at the given loading condition, with a beam wind: $\phi_{REF} = 2 \times \phi_{SE} + 5^\circ$.	
RPS	Range of positive stability for the ship at the given loading condition. If there is no down-flooding or other influences, this will be $\phi_{VS} - \phi_{SE}$.	RN c. 1900 van Harpen (7)
$RRPS$	The residual range of positive stability for the ship at the given loading condition, with a beam wind. The residual range is $\phi_{VS} - \phi_{SE}$, where ϕ_{VS} and ϕ_{SE} are defined for the wind lever applied.	BV1033 (8) van Harpen (7)
GZ_{30}	The righting lever arm of the ship at the given loading condition at a roll angle of 30° .	RN c. 1900
GZ'_{30}	The residual righting lever arm* of the ship at the given loading condition at a roll angle of 30° , with a beam wind.	
GZ_{40}	The righting lever arm of the ship at the given loading condition at a roll angle of 40° .	
GZ'_{40}	The residual righting lever arm* of the ship at the given loading condition at a roll angle of 40° , with a beam wind.	
GZ_{max}	The maximum righting lever arm of the ship at the given loading condition.	RN c. 1900 van Harpen (7)
GZ'_{max}	The maximum residual righting lever arm* of the ship at the given loading condition with a beam wind.	
$GZ'_{\phi_{REF}}$	The residual righting lever arm* at ϕ_{REF} for the ship at the given loading condition, with a beam wind.	BV1033 (8) van Harpen (7)
$GZ_{\phi_{SE}}$	The righting lever arm at ϕ_{SE} for the ship at the given loading condition, with a beam wind.	Sarchin (4)
$GZ_{\phi_{VS}}$	The righting lever arm at ϕ_{VS} for the ship at the given loading condition, with a beam wind.	
Continued on next page.		
*The residual righting lever arm is that portion of the righting lever in excess of the wind lever arm at that roll angle.		

Table 13. Stability Assessment Parameters from GZ Curve (Continued)		
Parameter	Description	Reference
$A_{\phi_{SE}-\phi_{VS}}$ $A'_{\phi_{SE}-\phi_{VS}}$	Total area under the GZ curve. The residual area [†] under the GZ curve.	CRN (14) BV1033 (8) van Harpen (7)
$A_{\phi_{SE}-30}$ $A'_{\phi_{SE}-30}$	The area under the GZ curve between ϕ_{SE} and 30°. The residual area [†] under the GZ curve between ϕ_{SE} and 30°.	IMO A167 (5)
$A_{\phi_{SE}-40}$ $A'_{\phi_{SE}-40}$	The area under the GZ curve between ϕ_{SE} and 40°. The residual area [†] under the GZ curve between ϕ_{SE} and 40°.	IMO A167 (5)
A_{30-40} A'_{30-40}	The area under the GZ curve between 30° and 40°. The residual area [†] under the GZ curve between 30° and 40°.	IMO A167 (5)
$A_{30-\phi_{VS}}$ $A'_{30-\phi_{VS}}$	The area under the GZ curve between 30° and ϕ_{VS} . The residual area [†] under the GZ curve between 30° and ϕ_{VS} .	
$A_{40-\phi_{VS}}$ $A'_{40-\phi_{VS}}$	The area under the GZ curve between 40° and ϕ_{VS} . The residual area [†] under the GZ curve between 40° and ϕ_{VS} .	
$A_{\phi_{SE}-\phi_{GZmax}}$ $A'_{\phi_{SE}-\phi_{GZmax}}$	The area under the GZ curve between ϕ_{SE} and ϕ_{GZmax} . The residual area [†] under the GZ curve between ϕ_{SE} and ϕ_{GZmax} .	
$A_{\phi_{GZmax}-\phi_{VS}}$ $A'_{\phi_{GZmax}-\phi_{VS}}$	The area under the GZ curve between ϕ_{GZmax} and ϕ_{VS} . The residual area [†] under the GZ curve between ϕ_{GZmax} and ϕ_{VS} .	
A_1	The residual area [†] under the GZ curve between ϕ_{SE} and ϕ_{VS} (assumes no down-flooding).	Sarchin (4)
A_2	The area above the GZ curve, and under the wind heeling lever arm curve for W knots, between ϕ_{SE} and $\phi_{SE} - \phi_{RB}$. ϕ_{RB} is a roll back angle.	Sarchin (4)
A_{ratio}	The ratio of areas A_1 / A_2 for the ship at the given loading condition with a beam wind.	Sarchin (4)
[†] The residual area under the GZ curve is the area above both the wind heeling lever arm curve and the $GZ = 0$ axis.		

The parameters in Table 13 are generated from calm-water (nominal or no wave) curves, as well as crest-balanced, trough-balanced, seaway-balanced (average of crest-balanced and trough-balanced) curves. Wind heeling lever arms corresponding to 50, 70, 90, and 100 knots were investigated.

Table 14. Ratios Derived from GZ Curves.

Parameter	Description	Reference
$\frac{GZ_{\phi_{SE}}}{GZ_{max}}$	Ratio of $GZ_{\phi_{SE}}$ with a 100 knot wind to GZ_{max} .	Sarchin (4)
$\frac{n000GZ_{max}}{t000GZ_{max} - c000GZ_{max}}$	Ratio of the maximum calm water righting lever to the difference between the maximum trough-balanced and crest-balanced levers. No wind levers applied.	
$\frac{n000A_{\phi_{SE}-\phi_{VS}}}{t000A_{\phi_{SE}-\phi_{VS}} - c000A_{\phi_{SE}-\phi_{VS}}}$	Ratio of the maximum area under the calm water GZ Curve to the difference between the maximum areas under the trough-balanced and the crest-balanced GZ Curves. No wind levers applied.	

Table 15 . Form Coefficient Assessment Parameters.

Parameter	Description
T	Mean draft (m)
KG	Vertical centre of gravity (fluid) (m)
Δ	Displacement in loading condition (tonnes)
L	Length on waterline (m)
B	Breadth on waterline (m)
f_m	Mean freeboard (m)
D	Mean depth, $(T + f_m)$ (m)
L/B	Length to beam ratio
KG/D	Ratio of KG over Mean depth
KG/B	Ratio of KG over Breadth on waterline
KG/T	Ratio of KG over draft
GM/B	Ratio of GM over Breadth on waterline
B_T	Waterline width at transom position (m)
B_T/B	Ratio of transom waterline width to maximum beam
C_B	Block coefficient
C_{WP}	Waterline coefficient
C_{WPA}	Aft waterline coefficient
C_{WPF}	Forward waterline coefficient
$C_{WPratio}$	Ratio of C_{WPA}/C_{WPF}
C_{VP}	Vertical prismatic coefficient
C_{VPA}	Aft vertical prismatic coefficient
C_{VPF}	Forward vertical prismatic coefficient
$C_{VPratio}$	Ratio of C_{VPA}/C_{VPF}
N_R	Number of rudders
A_{T_R}	Total rudder area (m ²)
R_t	Type of rudders (splayed = 0 vertical = 1)
A_{T_R}/A_V	Ratio of total rudder area to lateral area ($L \times T$)